

Super-Diffusive Behavior of Mobile Nodes and its Impact on Routing Protocol Performance

Sungwon Kim Chul-Ho Lee Do Young Eun
 Department of Electrical and Computer Engineering
 North Carolina State University, Raleigh, NC 27695
 {skim8, clee4, dyeun}@eos.ncsu.edu

Abstract—Mobility is the most important component in mobile ad-hoc networks (MANETs) and delay-tolerant networks (DTNs). In this paper, we first investigate numerous GPS mobility traces of human mobile nodes and observe super-diffusive behavior in all GPS traces, which is characterized by a ‘faster-than-linear’ growth rate of the mean square displacement (MSD) of a mobile node. We then investigate a large amount of access point (AP) based traces, and develop a theoretical framework built upon continuous time random walk (CTRW) formalism, in which one can identify the degree of diffusive behavior of mobile nodes even under possibly heavy-tailed pause time distribution, as in the case of reality. We study existing synthetic models and trace based models in term of the capability of producing various degrees of diffusive behavior, and use a set of Lévy walk models due to its simplicity and flexibility. In addition, we show that diffusive properties make a huge impact on contact-based metrics and the performance of routing protocols in various scenarios and that existing models such as random waypoint, random direction model or Brownian motion lead to overly optimistic or pessimistic results when diffusive properties are not properly captured. Our work in this paper thus suggests that the diffusive behavior of mobile nodes should be correctly captured and taken into account for the design and comparison study of network protocols.

Index Terms—Mobility models, trace-based models, super-diffusion, mobile ad-hoc networks, routing protocols

I. INTRODUCTION

Mobility is the most important factor in mobile ad-hoc networks (MANETs) and delay-tolerant networks (DTNs), and has posed serious challenge to the analysis and design of protocols on such networks. The mobility pattern directly impacts time-varying contact/inter-contact dynamics among mobile nodes, which in turn affect the performance of any protocol built over these mobility patterns [1]. Mobility models that fail to capture key characteristics in the movement pattern of mobile nodes will result in misleading guidelines on the design of new protocols and their performance evaluations and thus prevent us from making a right decision on our choice.

To cope with the issue above, numerous approaches have been put forth, ranging from various synthetic mobility modelings with certain desired properties, to the numerical study of MANET protocols using mobility traces obtained from real-world measurements. Synthetic mobility models [2], such as random waypoint models, random direction models, random walk or Brownian motion on a square or a sphere, and their variations, have been developed mainly for the purpose of simplicity and the ease of analysis, but subsequently been criticized for their unrealistic behaviors [3]. Another common approach is to rely on real mobility traces [4] and use them as inputs to a simulator for

the study and comparison of protocols [3], [5]. This approach, however, suffers from lack of the amount of available traces on a fine time/space scale; most existing traces show only partial or ‘filtered’ information about the real trajectories of mobile nodes such as access point (AP) association information or just contact duration with others, not the actual spatial-temporal information of the mobile users on a fine scale. While [3], [5] have tried to extract meaningful metrics and reconstruct detailed mobility patterns out of those filtered traces using some heuristic algorithms, such reconstructed traces are applicable only for the particular setting under consideration (e.g., the same campus) and are highly sensitive on the choice of the reconstruction algorithm.

In this paper, we take a different approach from the above two. We first investigate numerous GPS-based mobility traces as well as AP-based traces to find out key characteristics in movement patterns of mobile nodes. Unlike previous approaches using mobility traces, we specifically focus on the location of mobile nodes and how it changes over time. We then find that there is a common and distinctive characteristic observed in all mobility traces, *super-diffusive movement pattern*, which is characterized by a ‘faster-than-linear’ growth curve of the mean square displacement (MSD), i.e., $\mathbb{E}\{\|Z_t - Z_0\|^2\} \sim O(t^\gamma)$ with $\gamma > 1$, where $Z_t \in \mathbb{R}^2$ is the position of the mobile node at time t . The mean square displacement (MSD) – average square distance traveled by a mobile node over time duration t – is non-parametric and does not require any *a priori* specific mobility model for test, and is robust against the noise/error in the coordinates of mobile devices and the granularity of measurement time.

We then study existing synthetic models and trace based models to find out whether these models can produce varying degrees of super-diffusive behavior as observed from all GPS-based mobility traces as well as AP-based traces, and show that each model can generate only a limited range of diffusive properties or cannot be conveniently used to produce different degrees of diffusive property in practice. As a viable alternative, we use a set of Lévy walk models [6] as simple, easy-to-generate, yet still versatile mobility models. The Lévy walk model is an isotropic two-dimensional random walks, whose super-diffusive behavior (super-linear growth in MSD) is easily controlled via a single parameter – the exponent of its power-law step-length distribution.

In particular, for AP-based traces, we show that there is a way to extract diffusive property of mobile nodes in AP-based traces where location information Z_t of a mobile node is spatially quantized (to coordinates of APs) and sporadically time-sampled only when mobile nodes get inside the range of an AP. By capturing the tail behavior of the pause time of mobile nodes and with the help of continuous time random walk (CTRW) formalism,

we set out to extract key characteristics of the mobility patterns again from MSD measurements. Specifically, we analytically show that under the class of CTRW models, a class of Lévy walk models interspersed with power-law distributed pause time can easily capture diffusive behavior observed in various AP-based real traces. Lastly, we provide numerical results that show how varying degrees of diffusive properties affect the characteristics of several contact-based metrics and simulation results for network performance evaluation via six different routing protocols. We consider various scenarios by changing the resource constraints and node density, or by adding pause time. We also show the impact of diffusive property on network performance by using different diffusive sets of real trace. In particular, we show that existing models such as random waypoint models, random direction models and Brownian motion models may lead to overly optimistic or pessimistic results when diffusive properties are not properly captured. Our results thus collectively imply that correct diffusive behavior of mobile nodes should be taken into account for the development of new protocols and comparison with existing ones.

The rest of the paper is organized as follows. In Section II, we provide preliminary background and related work. In Section III, we investigate GPS mobility traces, and characterize the super-diffusive behavior of mobile nodes in terms of MSD. Then, we analyze existing mobility models in the context of their diffusive properties, and introduce Lévy walk models as good candidates for producing various degrees of diffusive behavior. In Section IV, we investigate AP-based traces, and characterize the diffusive properties when pause time is included. In Section V, we introduce CTRW and generalized MSD for a class of isotropic random walks with heavy-tailed pause time. In Section VI, we provide simulation and numerical results to show the impact of diffusive properties on contact-based metrics and network performance in various scenarios. In Section VII, we discuss the issue of other factors toward the super-diffusive property and how to incorporate the observed property in traces into the set of Lévy walk models. We then conclude in Section VIII.

II. PRELIMINARIES

In this section, we present background on the mean square displacement – a metric to capture the rate at which mobile nodes spread out, and the super-diffusion, and then give a brief summary of various approaches to the mobility modeling in the literature.

A. Mean Square Displacement (MSD)

One way to characterize the movement of a mobile node is to measure how far it is away from its current position after time t . This ‘diffusive’ behavior or the rate at which the mobile node spreads out can be described and quantified by so-called the mean square displacement (MSD) [6], [7]. Specifically, if we define $Z_t \in \mathbb{R}^2$ to be the position of the mobile node at time t , then the MSD becomes $M(t) \triangleq \mathbb{E}\{\|Z_t - Z_0\|^2\}$, (i.e., the second moment of the displacement $\|Z_t - Z_0\|$ between the current position at time t and the position at time 0) and $\sqrt{M(t)}$ gives typical amount of displacement of the mobile node after time t . For example, for a class of isotropic random walks with finite step-length¹ variance, the MSD will grow linearly with t , i.e., $M(t) \sim t$, provided that

¹Step-length is defined as the distance that a walker moves before changing its direction.

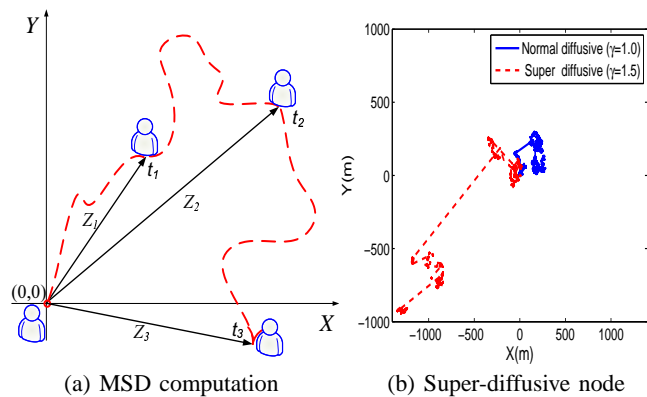


Fig. 1. MSD computation and sample trajectories of two nodes with different diffusive properties. Two nodes moving with the same speed (1.34 m/s) are simulated over the same duration (10000 sec).

the speed of the mobile node is $O(1)$ (or constant).² In general, we have $M(t) \sim O(t^\gamma)$ for some $\gamma > 0$. The slope of $M(t)$ in a log-log scale (γ) characterizes how fast a node spreads out in a simple way. Figure 1(a) shows how MSD can be measured. In this figure, as the mobile node starting from the origin follows the trajectory shown in dashed line, we can collect the displacement at each time instant t_i and investigate how MSD grows with time t to uncover the diffusive property of mobile nodes.

B. Super-Diffusion

When the step-length L has infinite variance ($\sigma_L^2 = \infty$), the mobile node tends to quickly spread out since longer step-lengths are generated more often. This behavior is called *super-diffusion* [8], [9], while for $\sigma_L^2 < \infty$ it is called normal diffusion. The varying degrees of diffusive properties of mobile nodes can be conveniently captured by the slope (γ) of $M(t)$ in a log-log scale (i.e., $M(t) \sim t^\gamma$). For example, we have $\gamma = 1$ for a normal diffusive case, while $\gamma > 1$ for super-diffusive case (faster-than-linear growth of the MSD). Figure 1(b) shows typical sample trajectories of two mobile nodes with different diffusive properties (different γ). While both nodes have the same speed (1.34 m/s) and run over the same duration (10000 sec), the super-diffusive node ($\gamma = 1.5$) spreads out from the origin much farther than the normal-diffusive node ($\gamma = 1.0$). As Figure 1(b) illustrates, the occasional long jumps are key characteristics of super-diffusive movement patterns.

C. Related Work

In the literature, numerous synthetic mobility models have been proposed to help network designers evaluate and compare protocols on MANETs and DTNs. Examples include random waypoint mobility model, random direction mobility model, random walk mobility model and its many derivatives such as Brownian motion model on a sphere, among others. (See [2] for a survey.) While these models are easy to generate and provide a quick platform to compare the performance of network protocols, they are mainly for the sake of simplicity and ease of comparison. Recent empirical results also indicate that current synthetic mobility models are not able to capture the characteristics of the real mobility patterns [10], [11].

²This is similar to the case of 2-D Brownian motion with its variance growing linearly with t .

On the other hand, a large set of traces measured in various environments [4], [12], [13] have been used to extract the key characteristics of mobile nodes and construct realistic mobility models [3], [5], [14], [15]. This collection of traces provides useful information when many participants are involved for a long observation period. In [3], [5], authors extract key features in mobile traces of their own campus, and propose realistic mobility models. [16] studied the time and space domain characteristics based on device registrations of mobile users at APs. In their extended work, *Model T* [14] included the space registration patterns of mobile users, and *Model T++* [15] incorporated both the time and space registration patterns in their model. [17] proposes a mobility model that features time variance and periodic reappearance in mobile traces. In [18], social network theory is employed to construct their community based mobility model and tested with real traces. In our work, we find ‘*super-diffusive movement patterns*’ in mobile traces as the key characteristic, and study other models in the view of producing diffusive properties.

The mobility model has also been a central topic in other scientific disciplines and various attempts to explain the movement of living organisms in nature have been made [19], [20], [21]. In particular, the so-called Lévy walk model, whose defining characteristics is its super-diffusive property, has been adopted for modeling the movement patterns of living organisms such as Microzooplankton [22], seabirds (albatross) [23], reindeer [24], jackals [25], and monkeys [26], [27], as well as capturing their foraging patterns [28], [29]. Quite recently, the super-diffusive behavior of mobile nodes has also received attention in representing human mobility pattern via a limited number of GPS-based traces [30], [31]. In contrast, in this paper, we investigate the vast amount of AP-based traces [4], [12], [13] (for which GPS-coordinate information is unavailable) through the CTRW formalism with heavy-tailed nodes’ pause time [3], and find that the super-diffusive behavior of nodes’ movement is a *universal* property in all the mobility traces under our study.

III. DIFFUSIVE BEHAVIOR IN GPS-BASED TRACES AND SYNTHETIC MODELS

In this section, we examine various GPS traces with different movement patterns and show all of them display the super-diffusive behavior. We then study whether the existing synthetic models can effectively capture the observed diffusive properties.

A. GPS Traces Validation

In this part, we investigate various GPS-based mobility traces for human beings and divide them into several categories based on the movement patterns – walking, running, inline skating and bicycling, in view of future applications such as MetroSense [32].

source	duration	sample	# of nodes
Web-Walking [33]	19 hours	3–60sec	11
Web-Running [33]	27 hours	3–60sec	22
Web-Inline Skating [33]	42 hours	3–60sec	17
Web-Bicycling [33]	36 hours	3–60sec	13
UW-Walking [4]	2 hours	1 sec	1
NCSU-Walking [35]	3 weeks	1 sec	1

TABLE I
SUMMARY OF GPS TRACES

1) *Available GPS Traces*: Table I is the summary of GPS traces of human beings under our consideration for their diffusive properties. Below is the detail about the GPS traces sources.

www.gps-tour.info: [33] is GPS device users’ community website where users share GPS traces. This website has an extensive amount of data from about 50 countries for various activities. We use this as our main source of GPS traces.

University of Washington: The GPS trace of University of Washington (UW) was collected by one of the authors in [34] for about two hours. This trace provides the x, y co-ordinates of the mobile node every second even inside of buildings by using Place Lab.

NCSU: NCSU GPS traces [35] were collected from the present authors’ school campus, where one student carried a GPS device (Garmin eTrex [36]) to collect GPS traces.

2) *Extracting MSD from GPS traces*: We investigate diffusive behavior of mobile nodes from all the available GPS traces in Table I. In order to decouple any effect of pause time from nodes’ diffusive behavior, we first removed all the pause time in the GPS traces, and then computed MSD from the resulting traces.

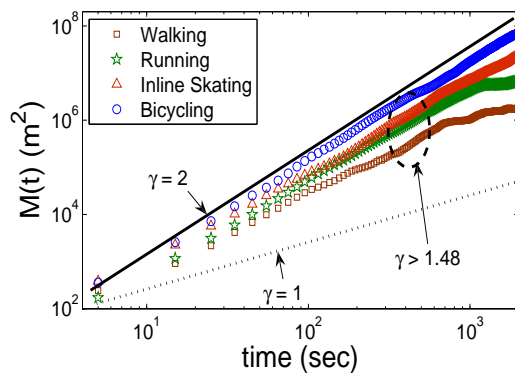


Fig. 2. MSD of human mobile nodes. In all cases, MSD increases faster than linear (super-diffusive behavior).

Figure 2 shows the MSD of mobile nodes with different movement patterns from GPS traces on a log-log scale. In all cases, MSD increases faster than linear with $\gamma > 1$, which implies the super-diffusive behavior of mobile nodes. Different values of γ conveniently captures the degree of diffusive behavior. For instance, mobile nodes with inline skate ($\gamma = 1.88$) tend to spread out quickly and show almost ballistic movements during certain time range, while walking mobile nodes ($\gamma = 1.48$) tend to spread out a little slower than mobile nodes with inline skate, but still faster than the normal diffusion with $\gamma = 1$ (the case of Brownian motion). Regardless of movement patterns, MSD grows faster than linear ($\gamma > 1$) in all cases.

B. Diffusive Behavior in Synthetic Models

In this part, we first study diffusive behavior in current synthetic mobility models via their MSD and show that most of them are not suitable for capturing varying degrees of super-diffusive pattern. We then propose to use a set of Lévy walk models as a simple alternative to current synthetic models.

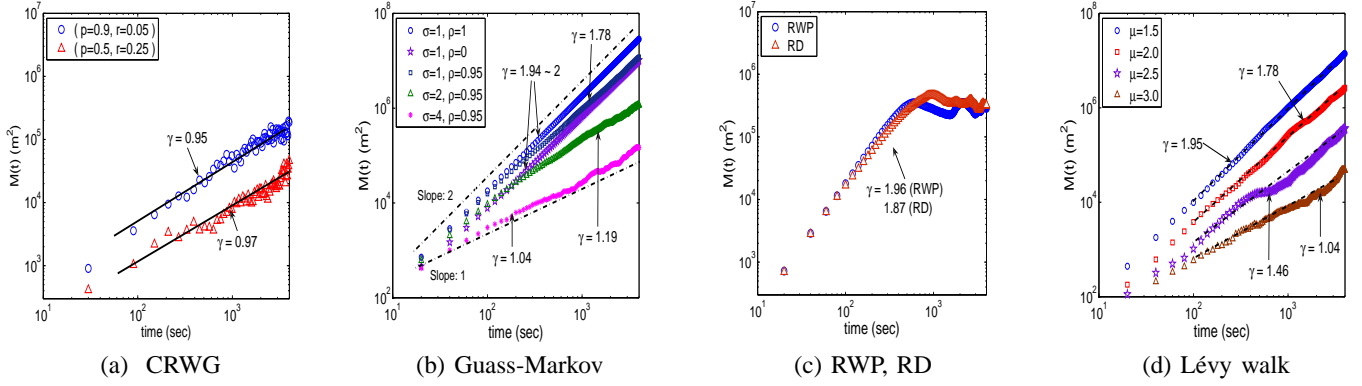


Fig. 3. Mean Square Displacement (MSD) of the existing synthetic mobility models (a)–(c) and the Lévy walk models on a log-log scale.

1) *Correlated Random Walks*: Among existing synthetic mobility models, we first consider several correlated random walk models to see if they can capture super-diffusive behavior. Since a mobile node in a correlated random walk tends to move along the same (or similar) direction for a while before changing its direction, these models might be good candidates for capturing super-diffusive behavior. Here, we consider the following set of correlated random walk models currently used in MANET simulations.

Correlated Random Walk on Grid (CRWG): A two-dimensional correlated random walk model on grid is proposed in [37] as a generalization of Manhattan mobility model [1]. In this model, a mobile node takes a step to the same direction as the previous one with probability p and opposite direction (moving backward) with probability q , while the probability of turning right or left is r satisfying $p+q+2r=1$. By assigning different values of p, q , we can control the degree of tendency for a mobile node to follow the same direction.

Gauss-Markov Mobility Model: A Gauss-Markov mobility model [2] first assigns an initial speed and direction of a mobile node. After moving for a fixed amount of time t , the mobile node updates its speed and direction based on the previous speed and direction (much like an auto-regressive recursion), where the speed and turning angle follow Gaussian distributions. Specifically, the direction (turning angle) of the n^{th} step θ_n is updated as

$$\theta_n = \rho\theta_{n-1} + (1-\rho)\bar{\theta} + \sqrt{(1-\rho^2)}\theta_{x_{n-1}}, \quad (1)$$

where $\theta_{x_n} \stackrel{d}{=} \mathcal{N}(0, \sigma^2)$ are *i.i.d.* zero mean Gaussian with variance σ^2 , $\rho \in [0, 1]$ is the correlation coefficient, and $\bar{\theta}$ is the preferred direction (angle). Step-length l_n also follows a similar recursion. We here consider a modified version of this Gauss-Markov model for fair comparison with other models in a way that after every t second, we update its step-length (instead of its speed) with its speed (1.34 m/s) and the preferred step-length (10m) kept the same all the time.

This Gauss-Markov model in (1) offers a great deal of flexibility by controlling the shape of distribution (σ) and correlation structure (ρ). For instance, when $\rho \approx 1$ and σ^2 is small, the turning angles (θ_i in Figure 4) remain almost the same, thus the mobile node will follow a straight line for a very long time, while for $\rho \approx 0$ and large σ the angle distribution approaches to a Gaussian with mean $\bar{\theta}$ and a large variance σ , but independent over time,

thus is close to that of an isotropic random walk.

2) *MSD of Correlated Random Walks*: Figure 3(a) shows the MSD of correlated random walks on grid (CRWG) using different model parameters on a log-log scale. For correlated random walks on grid (CRWG), we generate two sets of trajectories using parameters $(p, q, r) = (0.5, 0, 0.25)$ and $(p, q, r) = (0.9, 0, 0.05)$, respectively. The case of $p = 0.9$ reflects stronger correlations in the angles before changing the direction either to right or left, which can make the long jumps. Figure 3(a) shows that larger correlation coefficient with long steps only cause the MSD to move up, without affecting the linear growth of the MSD.

Figure 3(b) shows the MSD of Gauss-Markov mobility models with different degrees of correlations (ρ) and variance σ^2 of turning angle θ_n . For $\sigma = 2, 4$, a mobile node tends to deviate from its preferred angle with varying degree of step-lengths, which all contribute to the linear growth rate of the MSD even when there exists considerable amount of correlations $\rho = 0.95$. On the other hand, as can be seen for the case of $\sigma = 1$, Gauss-Markov model is likely to generate ‘ballistic’ trajectory ($\gamma = 2$) where the marginal angle distribution is ‘pointed’ with small σ (the mobile node has favorite direction and remembers this forever), and the MSD now grows much faster than linear. In all cases we see that σ plays a dominant role in shaping the angle distribution than the amount of correlation ρ , since the effect of small σ persists in the turning angle (the mobile node remembers its preferred angle forever) while the effect of correlations will be smoothed out over longer period as already seen in Figure 3(a).

To sum up, in order to capture the super-diffusive behavior with correlated walk models, one would have to tweak the distribution and correlations of the angles very carefully. As Figures 3(a) and 3(b) show, however, this approach would typically result in either $\gamma \approx 1$ or $\gamma \approx 2$, thereby making it unwieldy or practically infeasible to generate various mobility patterns with different degrees of diffusive behavior.

3) *MSD of mobility models with boundary (RWP and RD)*: The MSD of RWP (Random Waypoint) and RD (Random Direction) model as shown in Figure 3(c) illustrate the unique diffusive properties of these models. In both models, a node tends to spread out quickly from its initial position with the start of simulation. This gives rise to super-diffusive movement patterns due to ‘ballistic’ trajectories over a short period, during which the slope of MSD is almost $\gamma \approx 2$. By the time at which most nodes ‘feel’ the boundary of simulation, nodes tend to change

their directions and come back. Note that the timescale over which the node diffuses is much shorter than other models in Figure 3.

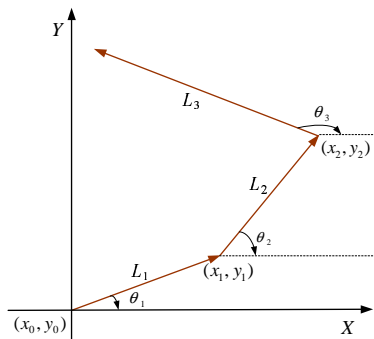


Fig. 4. Isotropic random walk with step-length L_i and turning angle θ_i . $\{L_i\}$ are *i.i.d.* with probability density $f_L(l)$, and $\{\theta_i\}$ are *i.i.d.* with $\text{unif}[0, 2\pi]$.

4) *Lévy Walk model*: A Lévy walk model is defined as follows. Suppose that a mobile node first chooses a step-length L and then moves that distance with some constant speed at an angle θ drawn uniformly and randomly from $[0, 2\pi]$ as illustrated in Figure 4. When it finishes that step-length, it repeats the process, independently of the past. When the first or the second moment of the step-length L becomes infinite, the model is called a *Lévy walk* [6]. For a Lévy walk model, the step-length density is characterized by

$$f_L(l) \sim l^{-\mu}, \quad 1 < \mu < 3,$$

where $\mu > 1$ is required for any valid probability density function. Under a Lévy walk mobility model, a mobile node occasionally moves along a very long straight line with non-negligible probability, interspersed with successive short steps with random orientation. Unlike other mobility models that would require subtle choice of several parameters to control diffusive properties, Lévy walk models can directly control the degree of super-diffusive properties by adjusting the exponent of step-lengths μ (single parameter) as shown in Figure 3(d).

IV. DIFFUSIVE BEHAVIOR IN AP-BASED TRACES

In addition to the GPS traces in Section III-A, there exist a large amount of mobility traces [4], [12], [13] with many mobile nodes recorded over much longer duration. These traces have been valuable resources and widely used in many studies of MANETs [5], [10], [38]. Unfortunately, however, they only provide ‘filtered’ information on the location of mobile nodes (AP association information [4], [12], [13] or duration of contact/inter-contact with other mobile nodes [4]) without exact movement patterns of mobile nodes. This prevents us from directly applying the same techniques used in Sections III-A to find diffusive behavior in mobile nodes. In addition, the long (heavy-tailed) pause time of mobile nodes in AP-based traces further complicates our understanding of their correct diffusive behavior purely from the movement components. In this section, we closely investigate AP-based traces in light of the MSD of mobile nodes and their pause times inside APs. Later in Section V, we will apply the CTRW formalism to make statistical inference about the true diffusive properties of mobile nodes in these traces.

A. Available AP-Based Traces

To verify diffusive properties in AP-based traces, we use two sets of data, University of California at San Diego (UCSD) traces [12] and Dartmouth College traces [4], for which AP-coordinates are available and they are most widely used in literatures. The summary of AP-based traces is given in Table II.

source	UCSD [12]	Dartmouth [4]
duration	1 month (2004.9~10)	6 months (2004.1~6)
# of nodes	275	13871
# of APs	196	506
sample	every 20 sec	depending on devices
place	campus	campus
area	1200m × 1400m	600m × 700m
device	PDA	various

TABLE II
SUMMARY OF AP-BASED TRACES

To extract the data set that can well represent the mobility of nodes from the huge amount of traces in Table II, we preprocessed the raw data. First, we used only weekday traces as the quantity of weekday traces is guaranteed to be large, and the mobility pattern during weekday is more consistent. Then, we considered the traces only after 9AM each day, as most mobile nodes start doing activities over this period. In order to rule out short-lived nodes leaving the network quickly, we only considered mobile nodes whose traces are at least 3 hours long.

B. MSD with Pause Time in AP-Based Traces

While AP-based traces do not have exact coordinates of mobile nodes, they still contain some information on how quickly mobile nodes spread out. Recall that for each mobile node and for each AP with known coordinates (x_i, y_i) , we know when the mobile node enters this AP (say, t_j). By tracking this information of time instants and coordinates in an increasing order of t_j , we can compute the distance a mobile node has traveled from its starting point for certain time duration. In other words, we can obtain sample values of the MSD and consequently its slope (γ) on a log-log scale.

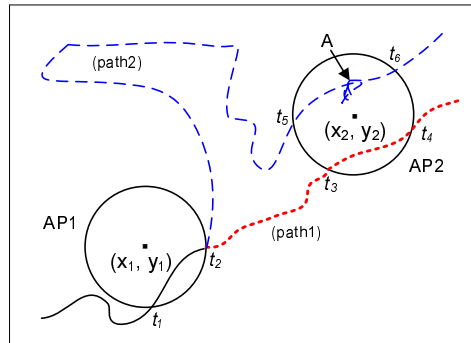


Fig. 5. Illustration of properties/limitations of AP-based traces. Location of mobile nodes are mapped to AP-coordinates whenever they are associated with APs and unknown otherwise. A is the location where a mobile node pauses.

In addition to the MSD samples, AP-based traces also contain some information about the pause time of each mobile node.

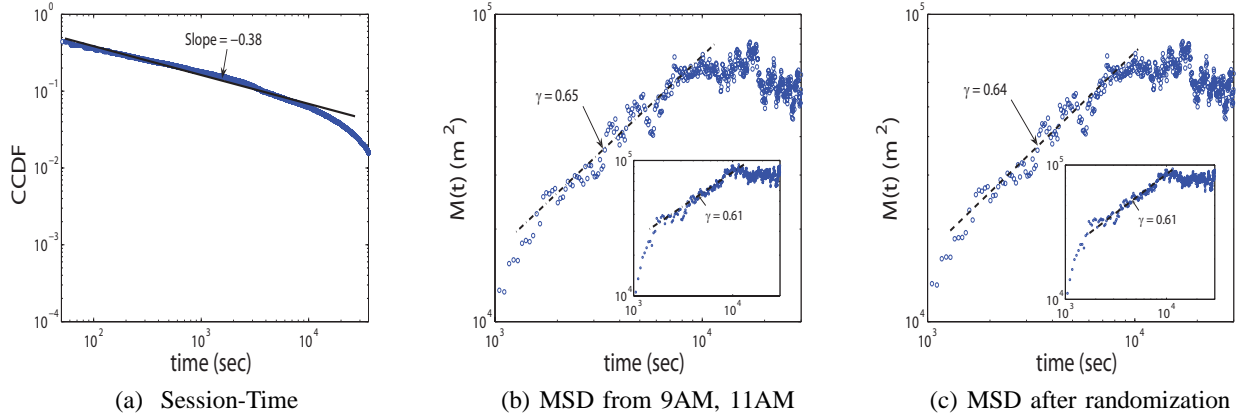


Fig. 6. UCSD Traces: (a) CCDF of session time ($\mathbb{P}\{T_{\text{session}} > t\}$); (b) MSD (from 9AM) on a log-log scale. The inset is for the trace that started from 11AM. Power-law density of T_{session} implies that T_{pause} also follows a power-law with the same exponent, making the MSD grow very slowly; (c) MSD after randomization of location of mobile nodes inside APs. The MSD exponents remain untouched after randomization when compared with Figure 6(b).

As shown in Figure 5, a collection of intervals during which a node is associated with some AP (e.g., $[t_1, t_2], [t_3, t_4], \dots$), tells us how long the node stays inside the range of an AP. This interval is often called a session time [3]. Note that one session time interval consists of actual amount of pause time (point A in AP2 in Figure 5) and the amount of time during which the mobile node keeps moving within the range of AP, i.e., $T_{\text{session}} = T_{\text{pause}} + T_{\text{move}}$. AP-based trace data reveal that the session time can be very long and range up to several hours [3] (e.g., students stay inside a classroom or library). Thus, it is reasonable to assume that pause time accounts for the majority of the session time interval, as long as the radius of ‘AP-disk’ is not so large.³

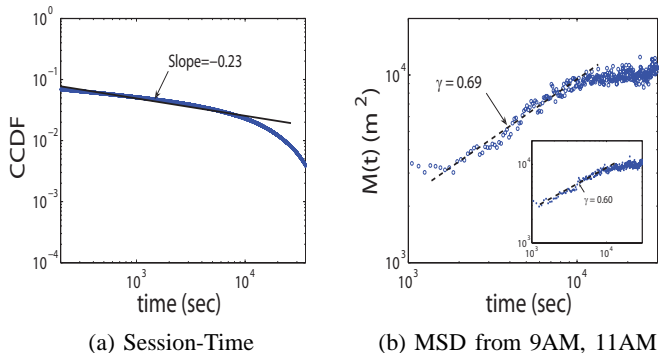


Fig. 7. Dartmouth Traces: (a) CCDF of session time; (b) MSD on a log-log scale. Session time and diffusive behaviors are similar to those of UCSD traces in Figure 6.

Figure 6(a) shows that the CCDF of the session time in UCSD trace data follows a power-law with exponent around -0.38 . The session time in Figure 6(a) is collected during the same period as in Figure 6(b). In these figures, we only consider session time samples up to 10 hours long, since the session time longer than 10 hours would be from devices that remain on but are not used for a long time. Note that the amount of sojourn time inside an AP due to movement (T_{move}) has the same order as the first

³A survey in [39] shows that the ratio between total moving time and total pause time (stationary time) of students in campus is about 0.12, implying that they spend on pause about 8 times more than on movement.

hitting time of a 2-D random walker to the perimeter of AP-disk starting from inside, whose distribution is known to be at most exponential [40]. This implies that the tail of the pause time probability density function $\phi(t) \sim t^{-\beta}$ with $\beta \approx 1.38$.

Figure 6(b) shows the sample values of the MSD $M(t)$ over time t in a log-log scale using traces from 9AM. (All the inset figures are from 11AM.) During the time duration from 2000 to 10000 seconds (for about 2.5 hours), MSD of mobile nodes increases with $\gamma \approx 0.65$. As expected, the existence of heavy-tailed pause time makes the MSD grow much slower compared with the case of GPS traces in Section III-A.⁴ Unlike the GPS traces, however, it is impossible to extract the pause time component from the AP-based traces as mobile nodes do move around inside APs, whose component is subsumed into the session time as a whole. Nevertheless, later in Section V, we will show that there is a way to infer the true diffusive behavior of mobile nodes from their movement components only and that it is again super-diffusive as is the case for GPS traces in Section III-A.

Here we point out that the super-diffusive behavior captured by the super-linear growth of $M(t)$ should be addressed only on a relevant time scale, not necessarily over all time t . For example, mobile nodes in school (students) spread out for a while and eventually tend to come back to their starting points (e.g., dormitory, library or classroom). Indeed, Figure 2 shows that the typical timescale for the super-diffusive behavior is up to $O(10^3)$ seconds, beyond which the mobile nodes display no further diffusive behavior or strong tendency to come back. Note that this timescale of several thousands of seconds is *without* the pause time, so with possibly very long pause time (e.g., several hours), the timescale for the diffusive behavior with pause time would have been prolonged. In both UCSD and Dartmouth traces, similar diffusive properties are observed in almost identical time scale $2000 \leq t < 10000$ as shown in Figures 6(b) and 7(b). Note that the time scale $2000 \leq t < 10000$ can represent the overall diffusive property well since both movement diffusive property and pause time are fairly considered in this time scale regardless of the type of mobile devices. We also point out that the diffusive property over time scale $t < 2000$ and $t \geq 10000$ is sensitive to the

⁴When MSD grows slower than linear ($\gamma < 1$) as shown in Figure 6(b), it is called ‘sub-diffusive’[19].

types of devices and user characteristics of traces. For example, PDA users are likely to start to move after they turn on the device, while laptop users⁵ tend to stay where they are right after they turn on the devices, which explains the different diffusive property for $t < 2000$. Beyond 10000 seconds, MSD tends to decrease or fluctuate around some value in both traces, which is due to the geographical constraints and/or the tendency of coming back to the starting point. However, note that the tendency of coming back to the same location that they have left in the morning for UCSD trace is stronger than Dartmouth trace, (All the users in UCSD traces are freshmen and most of them live in a dormitory.) which corresponds to the different diffusive property over $t \geq 10000$.

In AP-based traces, since the exact coordinates of mobile nodes at each time t is unavailable inside APs, we have simply assumed that the coordinate of an AP represents that of all mobile nodes within the communication range of APs. To justify this assumption, we did a simple experiment. First, we set the communication range r of one AP to $25m$, which is reasonable considering the real wireless network. Then, we newly set the coordinate of each mobile nodes inside an AP to another randomly (and uniformly) chosen location inside the AP-circle of radius r . Figure 6(c) shows the MSD $M(t)$ over time t after we randomize the locations of mobile nodes inside APs. Observe that the MSD exponents are largely unaffected by this randomization when compared with the original (non-randomized) version in Figure 6(b). To explain this behavior, let Z_t be the original coordinate of a mobile node at time t and N_t be a stationary zero-mean random process in 2-D (independent of Z_t) with $\mathbb{E}\{\|N_t\|^2\} = \sigma_N^2 < \infty$, representing the ‘noise’ in the coordinates of mobile nodes in our randomization procedure. Then, the ‘estimated’ location at time t becomes $\tilde{Z}_t \triangleq Z_t + N_t$, whose MSD is in the form of

$$\tilde{M}(t) = \mathbb{E}\{\|Z_t + N_t\|^2\} = \mathbb{E}\{\|Z_t\|^2\} + \sigma_N^2 = M(t) + \sigma_N^2.$$

Since we are only interested in the growth rate of the estimated MSD (slope of $\tilde{M}(t)$ on a log-log scale), the effect of ‘random quantization’ of the coordinates is ruled out in estimating the diffusive behavior of the original, but unknown Z_t . This implies that our estimate of the diffusive property through MSD is robust against other types of noises such as frequent association changes between APs, which is known as a *ping-pong transition* [41].

V. CONTINUOUS TIME RANDOM WALK (CTRW)

In Section IV, we showed diffusive properties of AP-based traces *as is*, with the pause time added. In this section, we introduce and utilize the general framework of CTRW [42], [43], [44] in order to uncover the true diffusive behavior of mobile nodes in AP-based traces without pause time. Specifically, we consider a class of isotropic random walks as depicted in Figure 4, but now we allow a mobile node to pause for a random amount of time with some probability p , independently of all others, at each turning point. Then, we present a set of equations to compute the MSD for this generalized CTRW (with heavy-tailed pause time) and identify under what conditions we can recover the observed the MSD growth rate of AP-based traces (as seen in Figures 6 and 7). Lastly, we confirm through theoretical and numerical results that a class of Lévy walk models interspersed with power-law

⁵Many different types of mobile devices contribute to Dartmouth trace. Even though laptop is not the only type of device in this trace, we use laptop users as an example to point out that users in Dartmouth trace are less mobile in general than the PDA users in UCSD trace over time scale $t < 2000$.

pause time can effectively capture the diffusive behavior observed in the ‘filtered’ AP-based traces.

TABLE III
NOTATIONS AND DEFINITIONS USED IN SECTION V

Notation	Definition
$M(t)$	mean square displacement (MSD)
$P(\vec{r}, t)$	joint probability density for a node to be located at $\vec{r} \in \mathbb{R}^2$ if started from the origin at $t = 0$
$f_L(l)$	probability density of a step-length
$\psi(t)$	probability density for the time duration of a single step
$f(\vec{r} t)$	conditional probability density that a node makes a displacement of \vec{r} in a single step for a given time duration t
$h(\vec{r}, t)$	joint probability density that a node makes a displacement of \vec{r} in a single step and this takes <i>exactly</i> t seconds ($h(\vec{r}, t) = f(\vec{r} t)\psi(t)$)
$H(\vec{r}, t)$	probability that a node makes a displacement of \vec{r} in time t <i>within</i> a single step and it takes <i>at least</i> t seconds to complete a single step ($H(\vec{r}, t) = f(\vec{r} t) \int_t^\infty \psi(\tau) d\tau$)
$\phi(t)$	probability density of a pause time between successive steps
$\Phi(t)$	probability that a node has not moved until time t ($\Phi(t) = \int_t^\infty \phi(\tau) d\tau$)
μ	step-length exponent
β	pause-time exponent
γ	MSD exponent

To set the stage, let $P(\vec{r}, t)$ be the joint probability density for a node to be located at $\vec{r} \in \mathbb{R}^2$ if started from the origin at $t = 0$. We define by $h(\vec{r}, t)$ the joint probability density that a node makes a displacement of \vec{r} in a single step and this takes *exactly* t seconds. We further define by $\phi(t)$ the probability density of a pause time between successive steps. In particular, $h(\vec{r}, t)$ can be written as $h(\vec{r}, t) = f(\vec{r}|t)\psi(t)$, where $\psi(t)$ is the probability density for the time duration of a single step and $f(\vec{r}|t)$ is the conditional probability density that a node makes a displacement of \vec{r} in a single step for a given time duration t . For example, if the node moves around with constant speed v all the time, then $f(\vec{r}|t)$ is in the form of $\delta(\|\vec{r}\| - vt)$ since the node can travel exactly vt meters during t seconds, where $\delta(\cdot)$ is the Dirac delta function.

Moreover, based on $h(\vec{r}, t)$ and $\psi(t)$, we further define $H(\vec{r}, t)$ and $\Phi(t)$. $H(\vec{r}, t)$ denotes the probability that a node makes a displacement of \vec{r} in time t *within* a single step and it takes *at least* t seconds to complete a single step (i.e., the probability that a node makes a displacement of \vec{r} for time t and it does not necessarily stop to initiate a new step or to stay at time t). Thus, $H(\vec{r}, t)$ can be written as $f(\vec{r}|t) \int_t^\infty \psi(\tau) d\tau$. In addition, $\Phi(t)$ denotes the probability that a node has not moved until time t , which is given $\int_t^\infty \phi(\tau) d\tau$. For reference, all the notations and definitions used in this Section are summarized in Table III.

We are interested in computing $P(\vec{r}, t)$ as this provides complete information on where the node will be located at any given time t . The desired $P(\vec{r}, t)$ can be obtained by summing over all the possible events. Note that a displacement of \vec{r} in time t can be made by either a single step or multiple steps. Thus, by conditioning upon first step taken, $P(\vec{r}, t)$ can be decomposed into the following four (disjoint) cases:

- (i) The node reaches \vec{r} in time t within its first step without pause during $[0, t]$.
- (ii) The node reaches \vec{r} at some earlier time $\tau \in (0, t)$ in its first step and stays there for a remaining time $t - \tau$ with probability p .
- (iii) The node reaches $\vec{\rho} \neq \vec{r}$ at some earlier time $\tau \in (0, t)$ in its first step, takes no pause time with probability $1 - p$, and

then continues to move from $\vec{\rho}$ to reach \vec{r} for a remaining time $t - \tau$.

- (iv) The node reaches $\vec{\rho} \neq \vec{r}$ at some earlier time $\tau' \in (0, t)$ in its first step, takes pause time of $\tau - \tau' > 0$ with probability p , and then continues to move from $\vec{\rho}$ to reach \vec{r} for a remaining time $t - \tau$.

Note that for cases (iii) and (iv), the node makes displacement of $\vec{r} - \vec{\rho}$ during $t - \tau$, which in turn consists of another several steps and pauses. Combining all the cases above, we arrive to the following recursive equation analogous to the backward equation of Chapman-Kolmogorov equation in the theory of Markov processes:

$$\begin{aligned} P(\vec{r}, t) &= H(\vec{r}, t) + \int_0^t d\tau h(\vec{r}, \tau) p \Phi(t - \tau) \\ &+ \iint_{\mathbb{R}^2} d^2\vec{\rho} \int_0^t d\tau h(\vec{\rho}, \tau) (1 - p) P(\vec{r} - \vec{\rho}, t - \tau) \\ &+ \iint_{\mathbb{R}^2} d^2\vec{\rho} \int_0^t d\tau \int_0^\tau d\tau' h(\vec{\rho}, \tau') p \phi(\tau - \tau') P(\vec{r} - \vec{\rho}, t - \tau), \end{aligned} \quad (2)$$

where $H(\vec{r}, t) = f(\vec{r}|t) \int_t^\infty \psi(\tau) d\tau$ and $\Phi(t) = \int_t^\infty \phi(\tau) d\tau$.

Note that as we are interested in the location \vec{r} of the node at any given time t , the node would be located at \vec{r} at time t during the movement of a single step or pause time, not necessarily to be the end of a single step or pause time. Thus, for the first and second terms, $H(\vec{r}, t)$ and $\Phi(t)$ are used instead of $h(\vec{r}, t)$ and $\phi(t)$, respectively.

As MSD is the second moment of the displacement $\|Z_t - Z_0\|$ between the current position at time t and the position at time 0 as defined before, Fourier transform (i.e., characteristic function) could be a convenient way to derive MSD. We define by $\overline{P}(\vec{\omega}, \cdot)$ the Fourier transform ($\vec{r} \rightarrow \vec{\omega}$) of $P(\vec{r}, \cdot)$, i.e., $\overline{P}(\vec{\omega}, \cdot) = \iint_{\mathbb{R}^2} P(\vec{r}, \cdot) e^{i\vec{\omega}\vec{r}} d^2\vec{r}$. Thus, MSD can be easily computed by taking the second derivative of $\overline{P}(\vec{\omega}, t)$ and by evaluating it at $\vec{\omega} = \vec{0}$, i.e.,

$$M(t) = - \left. \frac{\partial^2 \overline{P}(\vec{\omega}, t)}{\partial \vec{\omega}^2} \right|_{\vec{\omega}=\vec{0}}. \quad (3)$$

Similarly, we take Laplace transform with respect to t ($t \rightarrow s$) and define $\widehat{P}(\cdot, s) = \int_0^\infty P(\cdot, t) e^{-st} dt$. Note that we use \overline{F} and \widehat{F} to denote Fourier and Laplace transform of F with respect to ($\vec{r} \rightarrow \vec{\omega}$) and ($t \rightarrow s$), respectively. In particular, $\widehat{\overline{F}}$ is used to denote Fourier-Laplace transform of F over appropriate arguments. Note that Fourier and Laplace transforms exhibit the following convolution property:

$$\iint_{\mathbb{R}^2} \left[\iint_{\mathbb{R}^2} f(\vec{\rho}, \cdot) g(\vec{r} - \vec{\rho}, \cdot) d^2\vec{\rho} \right] e^{i\vec{\omega}\vec{r}} d^2\vec{r} = \overline{f}(\vec{\omega}, \cdot) \overline{g}(\vec{\omega}, \cdot),$$

and

$$\int_0^\infty \left[\int_0^t f(\cdot, \tau) g(\cdot, t - \tau) d\tau \right] e^{-st} dt = \widehat{f}(\cdot, s) \widehat{g}(\cdot, s),$$

where f and g are well-defined functions.

Therefore, by taking Fourier-Laplace transform of (2) and exploiting the efficiency of the convolutional property, we obtain

$$\begin{aligned} \widehat{\overline{P}}(\vec{\omega}, s) &= \int_0^\infty \left[\iint_{\mathbb{R}^2} P(\vec{r}, t) e^{i\vec{\omega}\vec{r}} d^2\vec{r} \right] e^{-st} dt \\ &= \widehat{H}(\vec{\omega}, s) + p \widehat{h}(\vec{\omega}, s) \widehat{\Phi}(s) + (1 - p) \widehat{h}(\vec{\omega}, s) \widehat{\overline{P}}(\vec{\omega}, s) \\ &\quad + p \widehat{h}(\vec{\omega}, s) \widehat{\phi}(s) \widehat{\overline{P}}(\vec{\omega}, s). \end{aligned} \quad (4)$$

Then, $\widehat{\overline{P}}(\vec{\omega}, s)$ becomes

$$\widehat{\overline{P}}(\vec{\omega}, s) = \frac{\widehat{H}(\vec{\omega}, s) + p \widehat{h}(\vec{\omega}, s) \widehat{\Phi}(s)}{1 - \widehat{h}(\vec{\omega}, s) [p \widehat{\phi}(s) + 1 - p]}. \quad (5)$$

In principle, it is theoretically possible to compute $P(\vec{r}, t)$ by taking inverse Fourier-Laplace transform of (5) as long as $h(\vec{r}, t)$ and $\phi(t)$ are known. However, the complicated structure of (5) defies any such attempt, and further, we are only interested in the behavior of MSD (3) in the asymptotic (large t). For this purpose, one can utilize the following Tauberian theorem [42], [45], which provides a relationship between large time t behavior of F and small s behavior of its Laplace transform \widehat{F} .

Theorem 1: [Tauberian theorem in [42], [45]] If $f(t) \geq 0$, $f(t)$ is ultimately monotonic as $t \rightarrow \infty$, L is slowly-varying at infinity and $0 < \rho < \infty$, then each of the relations

$$\widehat{f}(s) = \int_0^\infty f(t) e^{-st} dt \sim L\left(\frac{1}{s}\right) s^{-\rho} \quad \text{as } s \rightarrow 0$$

and

$$f(t) \sim \frac{t^{\rho-1} L(t)}{\Gamma(\rho)} \quad \text{as } t \rightarrow \infty$$

implies the other. \square

In this way, we can obtain the following:

Theorem 2: Let $f_L(l) \sim l^{-\mu}$ and $\phi(t) \sim t^{-\beta}$ ($\mu, \beta > 1$) be the probability density of the step-length and pause time, respectively⁶. Then, under the aforementioned CTRW formalism, for $p = 0$ we have

$$M(t) \sim t^\gamma, \quad \gamma = \begin{cases} 1 & \text{if } \mu > 3, \\ 4 - \mu & \text{if } 2 < \mu < 3, \\ 2 & \text{if } 1 < \mu < 2, \end{cases}$$

and for $0 < p \leq 1$ we have

$\beta \backslash \mu$	$1 < \mu < 2$	$2 < \mu < 3$	$\mu > 3$
$1 < \beta < 2, \beta < \mu$	$2 + \beta - \mu$	$2 + \beta - \mu$	$\beta - 1$
$1 < \beta < 2, \beta \geq \mu$	2	N/A	N/A
$2 < \beta < 3$	2	$4 - \mu$	1
$3 < \beta$	2	$4 - \mu$	1

Proof: Since we are only interested in the asymptotic behavior of the MSD $M(t)$, without loss of generality, we can work with 1-D projection (onto x -axis) of the original 2-D CTRW. To see this, note first that $M(t) = \mathbb{E}\{\|Z_t\|^2\}$, where $Z_t = (\|Z_t\| \cos \theta_t, \|Z_t\| \sin \theta_t) \in \mathbb{R}^2$ is the position of a mobile node at time t and $Z_0 = (0, 0)$. Since each step length and angle in the 2-D random walk are *i.i.d.*, its projection onto x -axis is also *i.i.d.* with zero mean (θ_t is uniform over $[0, 2\pi)$) and the 1-D projection $\|Z_t\| \cos \theta_t$ also becomes a CTRW with the same pause time as in 2-D case. In particular, each step of this 1-D CTRW is symmetric and its MSD is given by $\mathbb{E}\{\|Z_t\|^2 \cos^2 \theta_t\} = M(t) \mathbb{E}\{\cos^2 \theta_t\} = \text{Const.} M(t)$, thus the MSD behavior of 1-D version is essentially the same as that of 2-D version. Therefore, it suffices to show the MSD behavior of 1-D version. We refer

⁶In the aforementioned CTRW formalism, $\psi(t)$ is used instead of $f_L(l)$. Thus, note that $\psi(t) \sim t^{-\mu}$ ($1 < \mu$) because $f_L(l) \sim l^{-\mu}$ and the time duration t of a single step is equal to the length l of the single step times some constant $1/v$.

to [43], [44] for the proof of 1-D version with either $p = 0$ or $p = 1$.

For $0 < p < 1$, we extend the proof of 1-D version with $p = 1$. As we deal with the 1-D symmetric CTRW, 2-D location term ($\vec{r} \in \mathbb{R}^2$) is simply changed by 1-D location term ($r \in \mathbb{R}$) in the predefined functions (i.e., $P(\vec{r}, t)$, $f(\vec{r}, t)$, $h(\vec{r}, t)$, and $H(\vec{r}, t)$) with an appropriate 1-D integral operation. Similarly, Fourier transform ($r \rightarrow k$) of $f(r)$ is also redefined as $\bar{f}(k) = \int_{-\infty}^{\infty} f(r) e^{ikr} dr$ and thus \bar{F} is used to denote Fourier transform of F with respect to ($r \rightarrow k$) instead of ($\vec{r} \rightarrow \vec{\omega}$). Recall that $P(r, t)$ (1-D version of $P(\vec{r}, t)$) (2) with respect to the node location) and its Fourier-Laplace transform $\hat{P}(k, s)$ determine the slope of MSD (γ) in the aforementioned CTRW formalism. Given that $\psi(t) \sim t^{-\mu}$ and $\phi(t) \sim t^{-\beta}$ ($\mu, \beta > 1$), the conditional probability density that a node makes a displacement of $r \in \mathbb{R}$ in a single step for a given time duration t , $f(r|t)$, is still unknown to derive $P(r, t)$ and $\hat{P}(k, s)$. However, due to the 1-D symmetry of CTRW, $f(r|t)$ can be written as $f(r|t) = \frac{1}{2}[\delta(r - vt) + \delta(r + vt)]$ [43], [44].

We can now completely derive $P(r, t)$ and $\hat{P}(k, s)$. Then, as discussed earlier, by taking the second derivative of $\hat{P}(k, s)$, we obtain the following equation of MSD in Laplace transform domain.

$$\begin{aligned} \widehat{M}(s) &= -\left. \frac{\partial^2 \hat{P}(k, s)}{\partial k^2} \right|_{k=0} \\ &= -\left. \frac{\partial^2}{\partial k^2} \left(\frac{\widehat{H}(k, s) + p\widehat{h}(k, s)\widehat{\Phi}(s)}{1 - \widehat{h}(k, s)[p\widehat{\phi}(s) + 1 - p]} \right) \right|_{k=0} \\ &= \frac{-s \left. \frac{\partial^2 \widehat{H}(k, s)}{\partial k^2} \right|_{k=0} - \left. \frac{\partial^2 \widehat{h}(k, s)}{\partial k^2} \right|_{k=0}}{s [1 - \widehat{\psi}(s) + p\widehat{\psi}(s)(1 - \widehat{\phi}(s))]} \end{aligned} \quad (6)$$

Note that because of the symmetric form of $f(r|t)$, $\widehat{M}(s)$ can be simplified as (6). Then, to compute the slope of MSD (γ), we can exploit the Tauberian theorem (Theorem 1), which provides a relationship between large time t behavior of $M(t)$ and small s behavior of its Laplace transform $\widehat{M}(s)$ (i.e., the slope of MSD (γ) is mainly determined by the exponent of s). From (6), we can deduce that p only contributes to the constant coefficient in $\widehat{M}(s)$, not the exponent of s . Therefore, since p is not related to the small s behavior of $\widehat{M}(s)$, after applying the Tauberian theorem (Theorem 1) to (6), we can finally confirm that the large time t behavior of $M(t)$ for $0 < p < 1$ is same as that of the case where $p = 1$. ■

Remark 1: Although this framework of CTRW is based on a constant speed v , it is possible to generalize into random speed V with a well-defined probability distribution by rewriting corresponding equations for $h(\vec{r}, t) = f(\vec{r}|t)\psi(t)$. □

Theorem 2 provides a convenient relationship among exponents in the tail distribution of involved quantities. Specifically, if $p = 0$ (no pause time), the exponent in MSD satisfies $\gamma \geq 1$ in any case. Since $\beta = 1.23 \sim 1.38$ and $\gamma \approx 0.65 \sim 0.69$ in both sets of UCSD and Dartmouth traces (see Figures 6 and 7), Theorem 2 readily shows that the step-length distribution should follow a power-law ($2 < \mu < 3$) under a class of isotropic random walks. Specifically, Theorem 2 gives us an estimate of the step-length exponent $\mu = 2 + \beta - \gamma = 2.54 \sim 2.73$.

We also provide the estimate of the step-length exponent μ , numerically. First, in accordance with the power-law tail in the

pause time from UCSD and Dartmouth traces, we choose the ccdf of the pause time as $\mathbb{P}\{T_{\text{pause}} > t\} = (t/10)^{-\beta+1}$ (defined over $t \geq 10$) with $\beta = 1.23 \sim 1.38$ as observed in Figures 6(a) and 7(a). As to the unknown step-length distributions, we choose a family of power-law distributions $\mathbb{P}\{L > l\} = l^{-\mu+1}$ (defined over $l \geq 1$) with different μ to see their effect on γ . As before, after each step, the node may pause with probability p or proceed to next step with probability $1 - p$. We denote this generalized CTRW as GCTRW(μ, β, p) (or a.k.a. Lévy walk with power-law pause time in case of $1 < \mu < 3$).

$p \backslash \mu$	1.5	2.0	2.5	3.0	4.0
0.05	1.92	1.73	1.08	0.45	0.48
0.1	1.92	1.59	0.82	0.49	0.49
0.2	1.88	1.01	0.72	0.47	0.48

(a) $\beta = 1.38$ as in UCSD traces

$p \backslash \mu$	1.5	2.0	2.5	3.0	4.0
0.05	1.92	1.18	0.81	0.30	0.39
0.1	1.92	0.97	0.70	0.33	0.38
0.2	1.86	0.88	0.65	0.31	0.38

(b) $\beta = 1.23$ as in Dartmouth traces

TABLE IV
ESTIMATED MSD EXPONENTS γ USING GCTRW(μ, β, p)

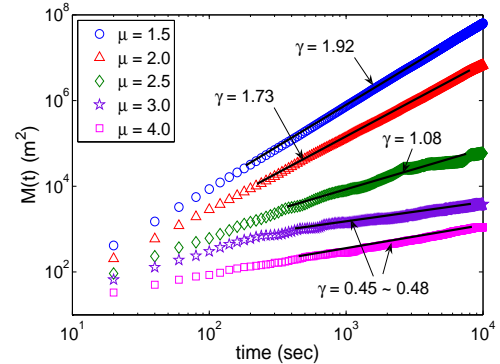


Fig. 8. MSD of GCTRW($\mu, 1.38, 0.05$) with $\mu = 1.5 \sim 4.0$

Tables IV (a) and (b) show numerically measured MSD exponents γ under GCTRW(μ, β, p) with different parameters. As an example, Figure 8 shows the MSD for GCTRW($\mu, 1.38, 0.05$) for different values of μ on a log-log scale. As shown in Table IV and Figure 8, the MSD grows faster with its exponent γ ranging from around 0.45 (for $\mu = 4.0$) to around 1.90 (for $\mu = 1.5$). In particular, when $\mu = 1.5$, γ is close to 2, implying that the strong power-law of the step-length distribution (with infinite mean in this case) dominates the diffusive behavior, notwithstanding the strong power-law of the pause time with $\beta = 1.23 \sim 1.38$. On the other hand, when μ is 3 or higher, which correspond to light-tailed step-length distribution with finite variance, γ remains around 0.45 without any noticeable change in the growth rate. When the step-length has infinite variance but finite mean ($2 < \mu < 3$), γ lies between the case of finite step-length variance ($\mu > 3$) and infinite mean step-length ($\mu < 2$). Throughout, different values of p have little effect on γ , since the power law structure of the 'effective' pause time T' (T with probability p and zero with

probability $1-p$) is mostly preserved. All numerical results show good match with Theorem 2.

Remark 2: While $GCTRW(\mu, \beta, p)$ entails power-law step-length distribution a priori, we admit the possibility that other factors such as strong correlations in angle and any other geometrical constraints may also lead to the observed diffusive behavior with desired value of γ . However, it is intractable to analytically show any relationship among those factors and the diffusive behavior. In contrast, we point out that our simple model based on generalized CTRW provides a clear-cut relationship as shown in Theorem 2 and offers an easy way to synthetically generate mobility traces with required diffusive behavior, which is an essential attribute for the design and performance study of network protocols. \square

VI. NUMERICAL RESULTS

In Section III and V, the super-diffusive movement patterns in mobile traces have been observed and estimated using the formulation of CTRW. The observation of super-diffusive property in mobile traces makes us wonder how these properties make an impact on networking performance. To find out how diffusive property affects interactions among nodes, we first present numerical results on contact-based metrics as contact is the most fundamental event that is related to dynamics among mobile nodes. Then, we provide the network performance of six different routing protocols (Direct Delivery [46], First Contact [47], Epidemic [48], Spray and Wait [49], PROPHET [50] and MaxProp [51]) by using Opportunistic Networking Environment (ONE) simulator [52].

A. Metrics

1) *Contact-based metrics:* In the performance evaluation of DTN routing protocols, ‘contact’ is the most important factor as nodes have an opportunity of sending and receiving packets only when they are within the transmission range with other nodes. We define that there is a ‘contact’ or they ‘meet’ when two nodes are within their common transmission range r . Among many contact-related metrics [53], we distinguish between the number of new contacts and total contacts among nodes. Below are the description of contact-based metrics used in this section.

- **The total number of new contacts:** Whenever a pair of nodes meet for the first time, this metric is incremented by one. Future contacts after the first meeting between this pair of nodes are not counted.
- **The total number of contacts:** Whenever any pair of nodes meet, this metric is incremented by one.

2) *Metric for the performance of routing protocol:* We use the message delivery ratio to assess the performance of routing protocols. This metric indicates the ratio of the number of successfully delivered messages to the number of messages sent by the sources.

B. Routing Protocol

In this part, we summarize the six routing protocols we consider in our performance evaluation. The full details of each routing protocol are in [46], [47], [48], [49], [50], [51]. In both Direct Delivery [46] and First Contact [47], there exists only a single copy of the message in the network. In Direct Delivery, the source forwards a message only when it meets the destination.

In First Contact, the source forwards a message to the first node it meets, and then that first node forwards the message only when it encounters the destination. In Epidemic [48], when two nodes meet, each node copies a message to the other (‘infect’) if the other node doesn’t have it already. After nodes exchange packets, they continue to receive packets that they do not have from other nodes. In Spray and Wait [49], it limits the number of messages it copies to other nodes. During spray phase, L copies are spread before it switches to the wait phase, which then performs Direct Delivery. In Binary Spray and Wait, which is a variant of Spray and Wait, half of copies are forwarded when a node encounters the other node until only single copy is left, and then it is switched to the wait phase. PROPHET [50] uses the node encounter history and transitivity to increase the performance. In MaxProp [51], the estimated probability of meeting every other node is exchanged to prioritize the packet exchange order. In addition, acknowledgements of delivered messages are transferred, so that the old messages are deleted in the network.

C. Simulation Setup

We use Opportunistic Networking Environment (ONE) simulator [52] for network performance evaluation. ONE simulator allows users to evaluate the DTN routing protocol performance easily using created scenarios in the simulator or reading external trace. Six well-known routing protocols summarized in Section VI-B are already incorporated in ONE simulator. Our simulation setup is as follows. 50 mobile nodes move around according to a given mobility model of our choice with constant speed (1.34 m/s) in an area ($1500m \times 1500m$). The source/destination nodes are randomly selected out of 50 nodes for each message (packet), and 400 messages are sent out for delivery during the simulation. We set the total simulation time to 4000 seconds and the maximum buffer size of each node to 500 messages. The message TTL is set to 4000 seconds. In Binary Spray and Wait, the number of message copies is set to 6, and in PROPHET, the delivery predictability transitivity scaling constant β , and the aging constant γ are set to 0.25 and 0.98, respectively. We gradually increase the ‘density’ of node coverage by changing their transmission range r from $25m$ to $200m$. For the underlying mobility model, as mentioned before, we use a set of Lévy walk models with different μ for the step-length distribution to reflect different degrees of diffusive behaviors. We also use RWP and RD as reference models and for comparison purpose. All simulation results are shown by averaging over 10 independent trials.

D. Impact of Different Diffusive Behavior

In this section, we investigate the impact of diffusive properties of mobile nodes on the contact-based metrics and the network performance of routing protocols. All the mobile nodes under consideration are assumed to follow the same mobility model of our choice.

1) *Contact-based Metrics:* Figure 9 shows how different diffusive properties make an impact on contact-based metrics. Note that the number of total contacts in Figure 9(c) is almost the same for RD model and all class of Lévy walk models with different diffusive behaviors under our consideration (γ ranges from 2 to 1, as μ increases from 1.5 to 3.0), except RWP model for the same transmission range r . However, the number of new contacts in Figure 9(a) shows the considerable differences with different

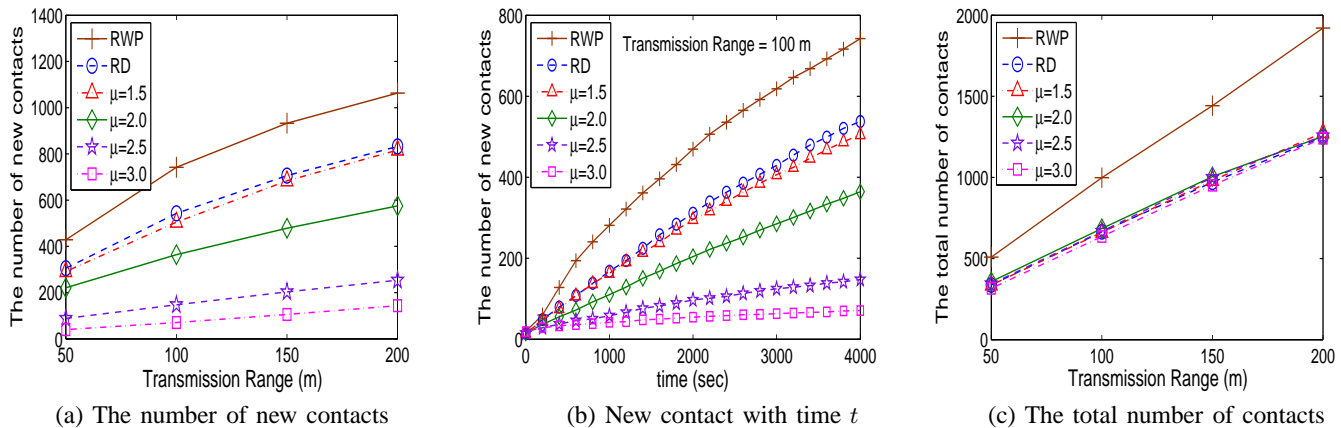


Fig. 9. Impact of diffusive properties on contact-based metrics: (a) total number of new contacts among all nodes after simulation time $t = 4000$ seconds; (b) total number of new contacts during time interval t ; (c) total number of contacts (including those among the same pair of nodes) after $t = 4000$ seconds. When μ is smaller (more frequent long steps), nodes tend to spread out further from the starting points, thus creating larger number of new contacts with other nodes.

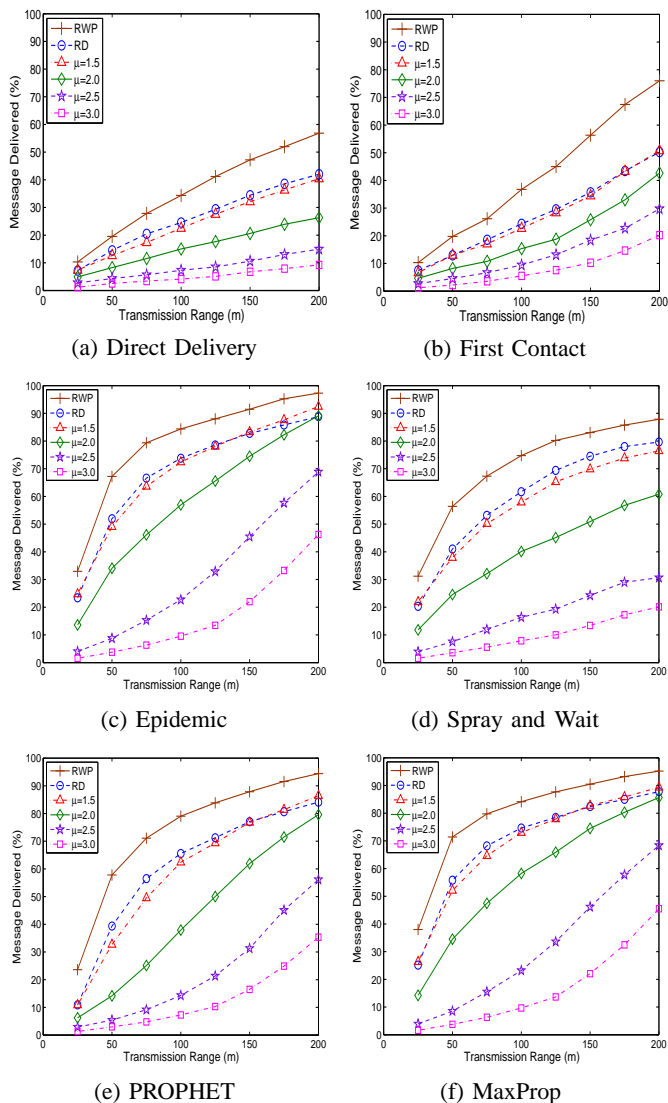


Fig. 10. Impact of diffusive properties on message delivery ratio for different routing protocols. As the nodes tend to diffuse faster (smaller μ), the message delivery ratio becomes larger. This tendency holds for the performance of all six routing protocols.

diffusive properties. In addition, Figure 9(a) also reveals that (i) when mobile nodes diffuse faster (smaller μ , or equivalently, larger γ), they are more successful in encountering new nodes, and (ii) for mobile nodes with larger μ (diffuse slower), most of their contacts are with the same nodes nearby (since the total number of contacts are the same from Figure 9(c)). Figure 9(b) further supports this observation; mobile nodes with faster diffusive property keep reaching out and meet more new nodes as time goes on. The number of new contacts for faster-diffusive nodes increases sharply, while nodes with slower-diffusive behavior (e.g., $\mu = 3.0$) rarely meet new nodes during the simulation time ($t = 4000$ seconds).

2) *Performance of Routing Protocol:* Figure 10 shows the average message delivery ratio of a class of Lévy walk models with different μ , RWP and RD model for each routing protocol. As can be seen clearly, varying degrees of diffusive behavior (parameterized by μ) result in widely different network performance. In particular, we see that faster diffusive behavior of mobile nodes (smaller μ) gives higher delivery ratio under the same transmission range. This is largely due to the increase in the number of new contacts with other mobile nodes for smaller values of μ , as nodes tend to reach out more aggressively. RD model, which spreads out quickly in the given bounded area, shows almost the identical message delivery ratio with a Lévy walk with $\mu = 1.5$. Note that the ordering of message delivery ratio in Figure 10 is exactly the same as that of the number of new contacts shown in Figure 9(a).

3) *Performance with pause time:* In this part, we add pause time in movement of mobile nodes to consider more realistic scenario because pause time plays an important role in mobility. We use the generalized CTRW model $GCTRW(\mu, 1.38, p)$ introduced in Section V with $p = 0.1$, as well as RWP and RD models interspersed with heavy-tailed pause time (with exponent 1.38 as extracted from UCSD trace in Section IV) after each step in each of the models. Figure 11 shows that pause time leads to lower message delivery ratio for all routing protocols. In particular, the message delivery ratio of $\mu = 2.0$ with $p = 0.1$ displays the similar trend as that of $\mu = 2.5$ but with no pause time (shown in Figure 10) in most routing protocols. In other words, the pause time induces slower diffusion overall. Again, the performance

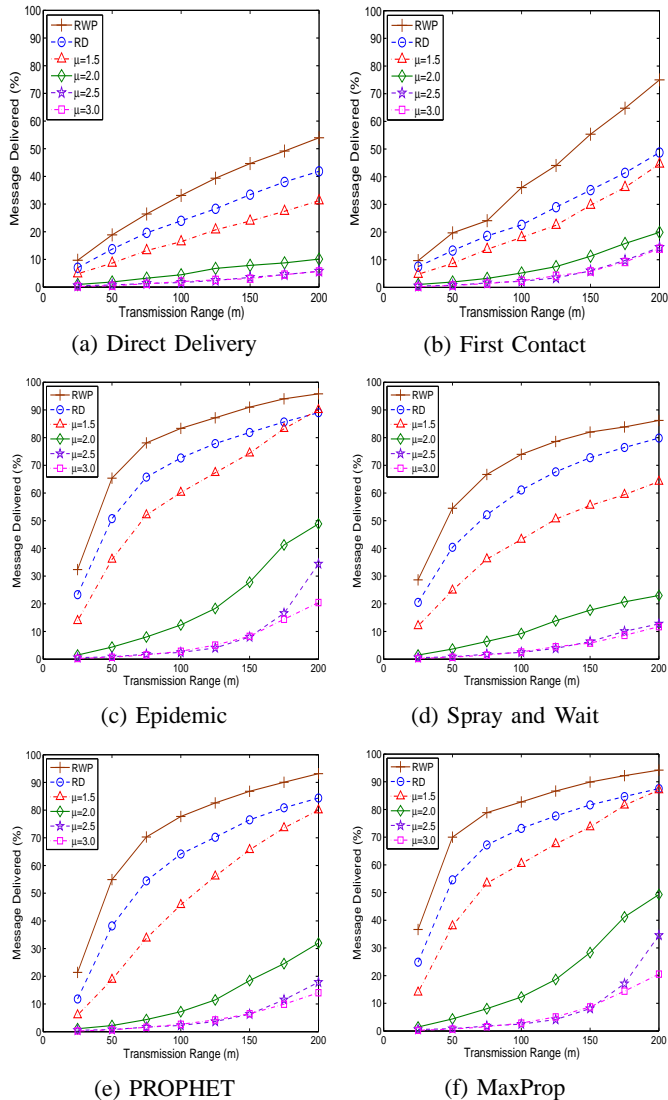


Fig. 11. Impact of diffusive properties on the performance of routing protocol with pause time considered. GCTRW(μ, β, p) model in Section V, along with RWP and RD are used. While pause time induces longer message delivery, the ordering of performance is preserved as before.

ordering in Figure 10 remains unchanged even with the addition of pause time. We also have evaluated the performance for larger p . The larger p induces slower diffusion, and leads to lower message delivery ratio as we can easily expect.

4) *Performance with different resource constraints:* For the performance evaluation in Section VI-D.2 and VI-D.3, we set message TTL and buffer size B to 4000 seconds and 500 messages respectively, which is basically no resource constraints. In this part, we investigate the performance evaluation with different resource constraints by changing message TTL and buffer size. We use epidemic routing protocol for performance evaluation, since most of routing protocols are variant of epidemic routing protocol with the performance trade off. By adjusting the message TTL and buffer size, we investigate how the resource constraints make an impact on network performance (message delivery ratio). We varies the message TTL from 750 to 1500 seconds and buffer size B from 200 to 300 (messages). Figures 12 and 13 show that the message delivery ratio always decreases as the resources gets

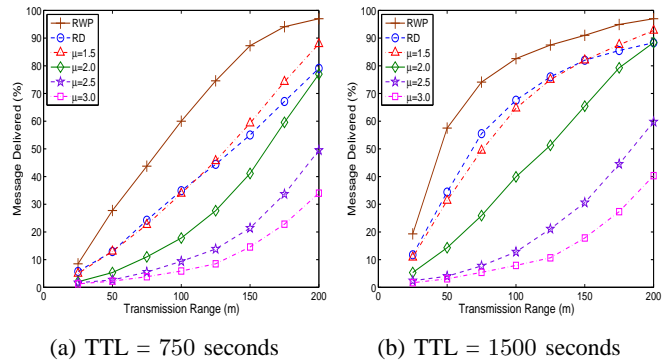


Fig. 12. Impact of diffusive properties on the performance of epidemic routing with different message TTL. The buffer size is set to 500 messages. The ordering of performance results in Figure 10 is preserved.

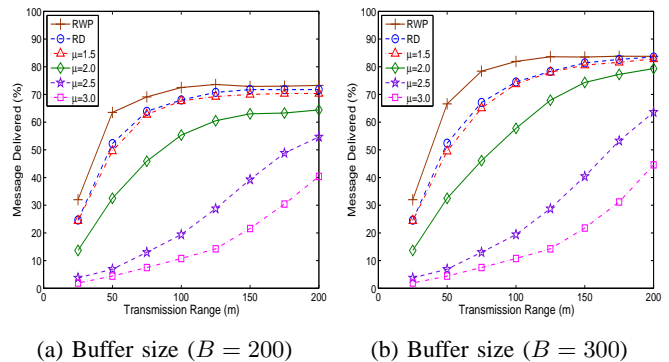


Fig. 13. Impact of diffusive properties on the performance of epidemic routing with different Buffer size B . The message TTL is set to 4000 seconds. The ordering of performance results in Figure 10 is preserved.

more limited. Still, we note that the ordering seen in Figure 10 is preserved in all cases.

5) *Performance with real trace:* In Section VI-D.2 and VI-D.3, we have shown the impact of diffusive properties on routing protocol performance for synthetic models with and without pause time. In this part, we show the impact of various diffusive properties on routing protocol performance via real traces. To this end, we divide the nodes in UCSD trace into two groups based on the number of AP changes for 4 hours (from 10 am to 2 pm). Specifically, if a node changes its AP for 4 hours at least 5 times, this node is in group A, otherwise it's in group B. We measured the MSD slope for nodes in groups A and B, which are 0.80 and 0.61, respectively. Since these traces are collected under the same geographic condition, we can show the impact of diffusive property on performance evaluation through real trace. The time duration of performance evaluation is 4 hours, and the message TTL is set to 3 hours. As shown in Figure 14, it turns out that the fast diffusive nodes (group A) show higher message delivery ratio (than those in group B) under all six routing protocols considered. This re-confirms the importance of diffusive property even under the realistic geographic settings in real trace (such as heterogeneous hotspot locations).

E. Performance Evaluation by Existing Mobility Models

Numerical results show diffusive properties make a huge impact on performance evaluation in DTN routing protocols. Note that existing models such as RWP, RD and Brownian motion ($\mu =$

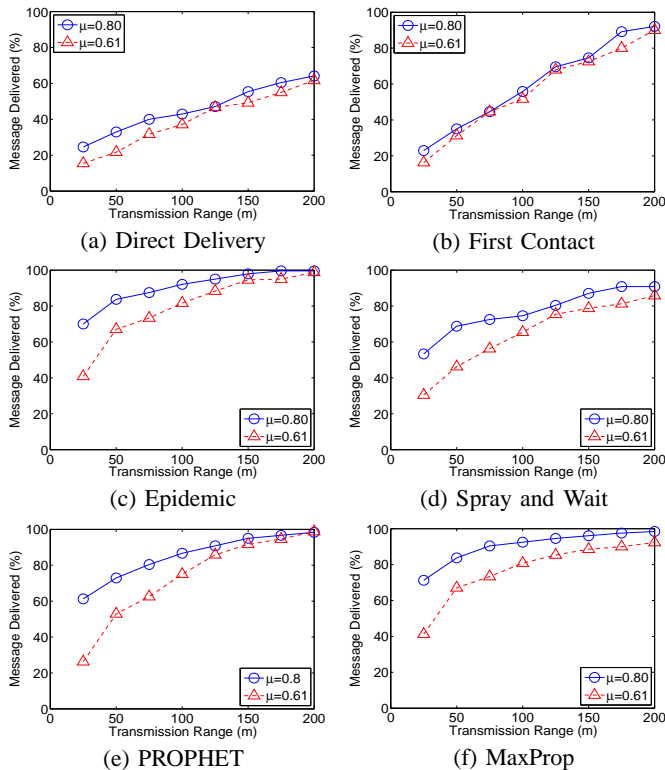


Fig. 14. Impact of diffusive properties on message delivery ratio for real trace. Faster diffusive ($\mu = 0.80$) nodes lead to higher message delivery ratio than slower diffusive ($\mu = 0.61$). Note that pause time is included for the MSD slope in real trace.

3.0) can predict misleading performance evaluation by being too optimistic or pessimistic. For example, mobile nodes in RWP model tend to move much more active than the real movements, and this may lead to better performance of routing protocol than real nodes can do. On the other hand, Brownian motion tend to stick to the same area and are not as active as the real nodes. This inactive mobility results in too pessimistic performance evaluation. These results can be also explained qualitatively by the mixing time [54]. In [55], [56], the authors used the mixing time as the time until a mobile node reaches its stationary distribution and claimed that “the larger the mixing time, the more localized the node movement, and it will take longer for a node to carry a message to a remote part of the network”. In our numerical results, we have shown that less diffusive movement such as Brownian motion leads to lower message delivery ratio over a given time frame. Similarly, in view of the mixing time argument in [55], [56], we can say that less diffusive movement such as Brownian motion is more ‘localized’ (slow mixing), which would translate into longer time for a message to get to its destination.

VII. DISCUSSION

So far we have observed that the super-diffusive property is universal in many real traces and has a significant impact on routing protocol performance under a wide range of scenarios. We have used a set of Lévy walk models to easily generate various degrees of diffusive properties. In this choice, the key contributing factor toward the super-diffusive property is the power-law distribution in the step-length as seen in Section V, but one can also ask if there exist other factors that may induce

the super-diffusive property. In addition, while we have mainly focused on the super-diffusive property of an *individual* mobile node, there have also been other important metrics such as the inter-meeting time between mobile nodes [57], [58], [59], which may equally impact the overall performance of any routing protocol. In view of these, in this section, we briefly discuss the issue of other factors toward the super-diffusive property and how to incorporate the observed inter-meeting time distribution from real traces into the set of Lévy walk models.

A. Other Factors Toward the Super-diffusive Property

In Section III-B, we studied whether existing synthetic models can capture different diffusive properties. We showed that a set of Lévy walk models can easily generate varying degrees of diffusive properties, and the power-law distribution in the step-length is the main factor of super-diffusive property in the class of 2-D isotropic random walk models. In this section we study if there exist other factors that also contribute to super-diffusive property by considering existing trace based models that feature non-isotropic, location-dependent preference in choosing the next destination. To this end, we consider *Model T* [14], which is a generic trace-based model built upon user registration patterns. Model T allows arbitrary choice of the distribution of AP locations and the popularity of each AP, so is more general than others in the literature [17], [39]. We have followed the trace generation procedure presented in [14], and the parameter settings are summarized in Table V⁷. In this section, we take the model T without the pause time for the sake of fair comparison with other models introduced in III-B.

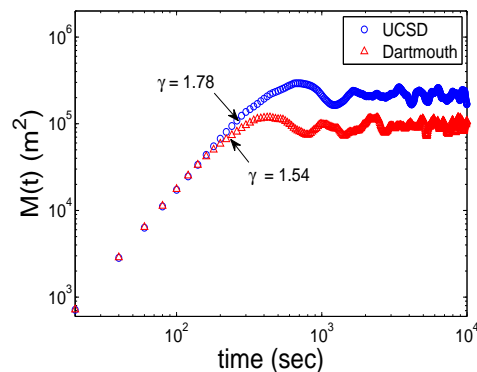


Fig. 15. MSD measurement under Model T [14]. The AP locations at UCSD and Dartmouth are used. This shows that trace based models can also lead to super-diffusive property of mobile nodes to some degree.

Figure 15 shows the measured MSD in a log-log scale as before, under the AP locations from UCSD and Dartmouth traces, respectively. It is clear that Model T can generate super-diffusive property, since the measured MSD slopes are greater than 1. We expect that this kind of MSD behavior is common to any other trace-based models relying on campus traces. A mobile node, from its starting point, tends to spread out quicker than normal diffusion as it typically moves towards its next location without much hesitation (wandering around like a pure Brownian motion), which is translated into the ‘diffusive regime’ ($\gamma > 1$) in the

⁷Weibull CDF equation $F(x) = 1 - e^{-(\frac{x}{a})^b}$ and exponential curve $y = p_1 e^{-p_2 x} + p_3$ have been used.

Parameters	Distribution	UCSD [12]	Dartmouth [4]
No. of APs		196	586
No. and distrib. of clusters	Weibull	a=2.649, b=1.253	a=6.561, b=1.253
No. of popular APs	Exponential	$p_1=0.691, p_2=0.332, p_3=0.250$	$p_1=0.726, p_2=0.217, p_3=0.232$
Intra-cluster transition prob.	Weibull para. a, b with Exponential	$p_{a1}=2.751, p_{a2}=0.631, p_{a3}=0.032$ $p_{b1}=1.255, p_{b2}=0.452, p_{b3}=0.361$	$p_{a1}=2.550, p_{a2}=0.544, p_{a3}=0.026$ $p_{b1}=1.211, p_{b2}=0.380, p_{b3}=0.355$
Intra-cluster trace length	Weibull	a=4.285, b=0.343	a=5.227, b=0.295
Inter-cluster transition prob.	Weibull	a=0.0078, b=0.3188	a=0.0069, b=0.2673
Inter-cluster trace length	Weibull	a=254.1, b=0.973	a=351.8, b=0.882

TABLE V
SUMMARY OF MODEL T PARAMETERS

early part of Figure 15. Once the mobile node has visited several locations, it then tends to move back and forth (with its own schedule, etc) in a constrained area, which corresponds to the ‘stationary regime’ ($\gamma \approx 0$) shown in later part of Figure 15. Note that the timescale of the diffusive regime will further extend (with smaller slope) when pause time is added as already shown in Figures 6 and 7.

Both trace-based models and the set of Lévy walks display super-diffusive property. In trace-based models such as Model T, the non-isotropic and location-dependent preference in choosing the next destination or other constraints (e.g., building locations) in underlying geometry collectively contribute toward the super-diffusive property. On the other hand, under the class of Lévy walk models the super-diffusivity is directly related with the exponent in the power-law step-length distributions even under possibly very strong pause time, as seen Section V. Thus, when it comes to the question of how to generate mobility scenarios for proper performance evaluations with super-diffusivity, both the trace-based models (e.g., Model T) and the class of Lévy walk models equally do well and should be preferred over any other synthetic models that do not capture super-diffusivity. Note that each of these choices has pros and cons. The former will be more suitable in capturing any geometric constraints and any unique feature inherent in the behaviors of participating mobile nodes, but makes it hard to analytically predict the degree of super-diffusivity as a function of all underlying information (e.g., AP locations and sizes, etc),⁸ while the latter lacks the precise realism but instead offers a very simple, parsimonious description of the model with a firm relationship among the few input parameters and the resulting degrees of diffusivity. This is precisely the reason why we have chosen to employ the Lévy walk models in demonstrating the importance of the super-diffusivity in mobility patterns as they give us convenient ways to tune the input parameters toward any desired degree of diffusive behavior, to the benefit of better prediction in performance evaluation and new protocol design.

B. Inter-meeting Time in Lévy Walk

Inter-meeting time between mobile nodes has been extensively considered in recent literature [57], [58], [59] as this governs how often mobile nodes meet for any chance of delivering packets to others. In particular, recent findings that the inter-meeting time distribution is close to a power-law up to some timescale followed by exponential fall-off [57], [58], [60] have become one of the key characteristics that any reasonable mobility scenario should

possess. We here maintain that the set of Lévy walk models can easily accommodate such properties of inter-meeting time distribution. First, we have already shown in Section V that any power-law pause time distribution can be incorporated into the Lévy walk model for precisely matching the required degree of super-diffusivity up to some relevant timescale (e.g., the early part of Figure 15)⁹. Then, to determine the transition point from power-law to exponential in the inter-meeting time distribution, we can apply the argument in [58], [60] where it is shown that the boundary size can be properly chosen (scaled) in conjunction with a given MSD of the mobile nodes (after the pause time is counted in) to match the transition point from power-law to exponential fall-off.

VIII. CONCLUSION

In this paper we have shown that super-diffusive behavior is the common characteristic in the movement of mobile nodes. We have investigated a large number of GPS-based traces as well as AP-based traces available in the literature. Our approach via the use of MSD coupled with CTRW formalism, allows us to statistically and theoretically identify the (possibly hidden) degree of diffusive behavior of mobile nodes. Our numerical results based on contact metrics and performance evaluation with six routing protocols show that diffusive property makes a huge impact on network performance. We expect that our initial study on the effect of mobile nodes’ diffusive behavior on the network performance opens up new possibilities toward better design of network protocols by uncovering super-diffusive nature observed in all the mobility traces.

ACKNOWLEDGMENTS

This work was supported in part by National Science Foundation under grants CNS-0831825, CCF-0830680, and CAREER Award CNS-0545893. The authors would like to thank the anonymous reviewers for their helpful suggestions and valuable comments that helped improve this work.

REFERENCES

- [1] F. Bai, N. Sadagopan, and A. Helmy, “Important: A framework to systematically analyze the impact of mobility on performance of routing protocols for adhoc networks,” in *Proceedings of IEEE INFOCOM*, San Francisco, CA, April 2003.

⁸The mathematical relationship between AP locations, their size, and the resulting MSD exponent is unknown and in general very hard to derive.

⁹While the theory in Section V is built upon asymptotical results for large time t , we observe that such asymptotical relationship quickly settles in for even small-to-moderate values of t as seen in Figure 8.

- [2] T. Camp, J. Boleng, and V. Davies, "A survey of mobility models for ad hoc network research," *Wireless Communications and Mobile Computing*, vol. 2, no. 5, pp. 483–502, 2002.
- [3] C. Tudeuce and T. Gross, "A mobility model based on WLAN traces and its validation," in *Proceedings of IEEE INFOCOM*, Seattle, WA, March 2005.
- [4] "CRAWDAD," in <http://crawdadd.cs.dartmouth.edu/>.
- [5] M. Kim, D. Kotz, and S. Kim, "Extracting a mobility model from real user traces," in *Proceedings of IEEE INFOCOM*, Barcelona, Spain, April 2006.
- [6] M. Shlesinger and G. Zaslavsky, *Levy Flights and Related Topics in Physics*. Springer, 1994.
- [7] H. Berg, *Random Walks in Biology*. Princeton University Press, 1983.
- [8] J. Klafter and I. M. Sokolov, "Anomalous diffusion spreads its wings," *Physica A*, vol. 117, no. 1, pp. 179–188, 1983.
- [9] E. Weeks, T. Solomon, and H. Swinney, "Observation of anomalous diffusion and Lévy flights," (Eds) *Lévy flights and related topics in Physics*, Springer, pp. 51–71, 1995.
- [10] A. Chaintreau, P. Hui, J. Crowcroft, C. Diot, R. Gass, and J. Scott, "Impact of human mobility on the design of opportunistic forwarding algorithms," in *Proceedings of IEEE INFOCOM*, Barcelona, Spain, Apr 2006.
- [11] T. Henderson, D. Kotz, and I. Abyzov, "The changing usage of a mature campus-wide wireless network," in *ACM Mobicom*, Philadelphia, PA, 2004.
- [12] M. McNett and G. M. Voelker, "Access and Mobility of Wireless PDA Users," UC San Diego, Tech. Rep., 2004.
- [13] "USC trace," in <http://nile.usc.edu/MobiLib/>.
- [14] R. Jain, D. Lelescu, and M. Balakrishnan, "Model T: an empirical model for user registration patterns in a campus wireless LAN," in *ACM Mobicom*, Cologne, Germany, 2005, pp. 170–184.
- [15] D. Lelescu, U. C. Kozat, R. Jain, and M. Balakrishnan, "Model T++: an empirical joint space-time registration model," in *ACM Mobicom*, Florence, Italy, 2006, pp. 61–72.
- [16] R. Jain, A. Shivaprasad, D. Lelescu, and X. He, "Towards a model of user mobility and registration patterns," in *ACM SIGMOBILE Mobile Computing and Communication Review*, 2004.
- [17] W. Hsu, T. Spyropoulou, K. Psounis, and A. Helmy, "Modeling time-variant user mobility in wireless mobile networks," in *Proceedings of IEEE INFOCOM*, Anchorage, Alaska, 2007.
- [18] M. Musolesi and C. Mascolo, "A community based mobility model for ad hoc network research," in *REALMAN*, Florence, Italy, May 2006.
- [19] J. Klafter, M. Shlesinger, and G. Zumofen, "Beyond Brownian motion," *Physics Today*, 1996.
- [20] M. Shlesinger, "Physics in the noise," *Nature*, vol. 411, 2001.
- [21] N. Chakravarti, "Beyond Brownian motion: A Levy flight in magic boots," *RESONANCE*, 2004.
- [22] F. Bartumeus, F. Peters, S. Pueyo, C. M. é, and J. Catalan, "Helical Lévy walks: Adjusting searching statistics to resource availability in microzooplankton," *Proceedings of National Academy of Science*, vol. 100, no. 22, pp. 12 771–12 775, October 2003.
- [23] G. Viswanathan, V. Afanasyev, S. Buldrev, E. Murphy, P. Prince, and H. Stanley, "Lévy flight search patterns of wandering albatrosses," *Nature*, vol. 381, no. 30, pp. 413–415, 1996.
- [24] A. Marell, J. Ball, and A. Hofgaard, "Foraging and movement paths of female reindeer: insights from fractal analysis, correlated random walks, and Lévy flights," *Canadian Journal of Zoology*, vol. 80, 2002.
- [25] R. Atkinson, C. Rhodes, D. Macdonald, and R. Anderson, "Scale-free dynamics in the movement patterns of jackals," *OIKIS*, vol. 98, pp. 134–140, 2002.
- [26] G. Ramos-Fernandez, J. Mateos, O. Miramontes, G. Cocho, H. Larralde, and B. Ayala-Ocozco, "Lévy walk patterns in the foraging movements of spider monkeys (ateles geoffroyi)," *Behavioral Ecology and Sociobiology*, vol. 55, pp. 223–230, 2004.
- [27] D. Boyer, O. Miramontes, G. Ramos-Fernandez, J. mateos, and G. Cocho, "Modeling the searching behavior of social monkeys," *Physica A: Statistical Mechanics and its Applications*, vol. 342, no. 1–2, pp. 329–335, Oct. 2004.
- [28] M. Shlesinger and J. Klafter, *On growth and form*. Martinus Nijhoff Publisher, 1986.
- [29] G. Viswanathan, S. Buldyrev, S. Havlin, M. da Luz, E. Raposo, and H. Stanley, "Optimizing the success of random searches," *Nature*, vol. 401, 1999.
- [30] S. Kim, C. Lee, and D. Y. Eun, "Super-diffusive behavior of mobile nodes from GPS traces," in *ACM Mobicom Poster*, 2007, available at "<http://www4.ncsu.edu/~skim8/trace/Mobicom07-poster-Kim.pdf>".
- [31] I. Rhee, M. Shin, S. Hong, K. Lee, and S. Chong, "Human mobility patterns and their impact on delay tolerant networks," in *Hot Topics in Networks (HotNets-VI)*, Atlanta, GA, Nov 2007.
- [32] "Merosense," in <http://metrosense.cs.dartmouth.edu/>.
- [33] "GPS Trace," in <http://www.gps-tour.info/>.
- [34] J. Kang, W. Welbourn, B. Stewart, and G. Borriello, "Extracting places from traces of locations," *ACM SIGMOBILE Mobile Computing and Communications Review*, vol. 9, pp. 58–68, July 2005.
- [35] "NCSU trace," in <http://www4.ncsu.edu/~skim8/trace/>.
- [36] "Garmin website," in <http://www.garmin.com/>.
- [37] S. Bandyopadhyay and E. Coyle, "Stochastic properties of mobility models in mobile ad hoc networks," in *Conference on Information Sciences and System(CISS)*, Princeton, NJ, 2006.
- [38] M. Kim and D. Kotz, "Modeling users mobility among WiFi access points," in *Proceedings of the International Workshop on Wireless Traffic Measurements and Modeling*, Seattle, WA, June 2005, pp. 19–24.
- [39] W. Hsu, K. Merchant, C. Hsu, and A. Helmy, "Weighted waypoint mobility model and its impact on ad hoc networks," *ACM Mobile Computer Communications Review*, January 2005.
- [40] S. Redner, *A guide to first-passage processes*. Cambridge University Press, 2001.
- [41] J. Lee and J. C. Hou, "Modeling steady-state and transient behaviors of user mobility: Formulation, analysis, and application," in *ACM Mobicom*, Florence, Italy, 2006.
- [42] B. D. Hughes, *Random Walks and Random Environments: I*. Oxford University Press, 1995.
- [43] J. Klafter and G. Zumofen, "Lévy statistics in a Hamiltonian system," *Physical Review E*, vol. 49, no. 6, pp. 4873–4877, June 1994.
- [44] G. Zumofen and J. Klafter, "Laminar-localized-phase coexistence in dynamical systems," *Physical Review E*, vol. 51, no. 3, pp. 1818–1821, March 1995.
- [45] W. Feller, *An Introduction to Probability Theory and its Applications II*. JWS, 1971.
- [46] T. Spyropoulos, K. Psounis, and C. Raghavendra, "Single-copy routing in intermittently connected mobile networks," in *SECON*, Santa Clara, CA, 2004.
- [47] S. Jain, K. Fall, and R. Patra, "Routing in a delay tolerant network," in *Proceedings of ACM SIGCOMM*, Portland, OR, 2004.
- [48] A. Vahdat and D. Becker, "Epidemic Routing for Partially-Connected Ad Hoc Networks," Duke University Technical Report CS-200006, Tech. Rep., April 2000.
- [49] T. Spyropoulos, K. Psounis, and C. Raghavendra, "Spray and wait: an efficient routing scheme for intermittently connected mobile networks," in *ACM Sigcomm workshop*, Philadelphia, PA, 2005.
- [50] A. Lindgren, A. Doria, and O. Schelen, "Probabilistic routing in intermittently connected networks," in *The First International Workshop on Service Assurance with Partial and Intermittent Resources (SAPIR)*, Fortaleza, Brazil, 2004.
- [51] J. Burgess, B. Gallagher, D. Jensen, and B. N. Levine, "MaxProp: Routing for Vehicle-Based Disruption-Tolerant Networks," in *Proceedings of IEEE INFOCOM*, Barcelona, Spain, April 2006.
- [52] A. Keranen, J. Ott, and T. Karkkainen, "The ONE simulator for DTN protocol evaluation," in *SIMUTools*, Rome, Italy, 2009.
- [53] A. Khelil, P. Maron, and K. Rothermel, "Contact-based mobility metrics for delay-tolerant ad hoc networking," in *International Symposium on Modeling, Analysis, and Simulation of Computer and Telecommunication Systems*, 2005, pp. 435–444.
- [54] D. Aldous and J. Fill, "Reversible markov chains and random walks on graphs. (monograph in preparation)," in <http://stat-www.berkeley.edu/aldous/RWG/book.html>.
- [55] T. Spyropoulos, A. Jindal, and K. Psounis, "An analytical study of fundamental mobility properties for encounter-based protocols," in *International Journal of Autonomous and Adaptive Communications Systems*, vol. 1, no. 1, 2008, pp. 4–40.
- [56] T. Spyropoulos, K. Psounis, and C. S. Raghavendra, "Efficient Routing in Intermittently Connected Mobile Networks: The Single-Copy Case," *IEEE Transactions on Networking*, vol. 16, no. 1, Feb 2008.
- [57] T. Karagiannis, J. L. Bourkec, and M. Vojnovic, "Power law and exponential decay of inter contact times between mobile devices," in *ACM Mobicom*, Montreal, Canada, 2007.
- [58] H. Cai and D. Y. Eun, "Crossing over the bounded domain: From exponential to power-law inter-meeting time in MANET," in *ACM Mobicom*, Montreal, Canada, 2007.
- [59] P. Hui, A. Chaintreau, J. Scott, R. Gass, J. Crowcroft, and C. Diot, "Pocket switched networks and the consequences of human mobility in conference environments," in *Proceedings of ACM SIGCOMM first*

workshop on delay tolerant networking and related topics (WDTN-05), Philadelphia, PA, 2005.

- [60] H. Cai and D. Y. Eun, "Toward stochastic anatomy of inter-meeting time distribution under general mobility models," in *ACM Mobihoc*, Hong Kong, China, 2008.



Sungwon Kim received the B.S. degree in Electrical Engineering from Ajou University, Suwon, South Korea, in 2003, and received the M.S. degree in Computer Engineering from North Carolina State University in 2006. Since 2006, he has been a Ph.D. student in the Department of Electrical and Computer Engineering at North Carolina State University, Raleigh, NC. His research interests include mobility modeling in mobile ad-hoc networks and delay tolerant networks.



Chul-Ho Lee received the B.E. degree with honors in Information and Telecommunication Engineering from Korea Aerospace University, Goyang, Korea in 2003 and the M.S. degree in Information and Communications from Gwangju Institute of Science and Technology (GIST), Gwangju, Korea, in 2005. Since August 2006, he has been a Ph.D. student in the Department of Electrical and Computer Engineering at North Carolina State University, Raleigh, NC. His research interests include wireless and mobile networks.



Do Young Eun received his B.S. and M.S. degree in Electrical Engineering from Korea Advanced Institute of Science and Technology (KAIST), Taejon, Korea, in 1995 and 1997, respectively, and Ph.D. degree in Electrical and Computer Engineering from Purdue University, West Lafayette, IN, in 2003. Since August 2003, he has been an Assistant Professor with the Department of Electrical and Computer Engineering at North Carolina State University, Raleigh, NC. His research interests include network modeling and analysis, mobile ad-hoc/sensor networks, congestion control, and resource allocation. He is a member of Technical Program Committee of various conferences including IEEE INFOCOM, ICC, Globecom, ICCCN, and ACM MobiHoc. He received the Best Paper Awards in the IEEE ICCCN 2005 and the IEEE IPCCC 2006, and the NSF CAREER Award 2006. He supervised and co-authored a paper that received the Best Student Paper Award in ACM MobiCom 2007.